JACS
JOURNAL OF THE AMERICAN CHEMICAL SOCIETY

Communication

Metal-Organic Framework with Dual Active Sites in Engineered Mesopores for Bioinspired Synergistic Catalysis

Yangjian Quan, Yang Song, Wenjie Shi, Ziwan Xu, Justin S Chen, Xiaomin Jiang, Cheng Wang, and Wenbin Lin

J. Am. Chem. Soc., **Just Accepted Manuscript** • DOI: 10.1021/jacs.0c02966 • Publication Date (Web): 25 Apr 2020

Metal-Organic Framework with Dual Active Sites in Engineered Mesopores for Bioinspired Synergistic Catalysis

Yangjian Quan,[†,§] Yang Song,[†,§] Wenjie Shi,[†,‡] Ziwan Xu,[†] Justin S. Chen,[†] Xiaomin Jiang,[†] Cheng Wang,[‡] and Wenbin Lin[†,*]

[†]Department of Chemistry, The University of Chicago, Chicago, IL 60637, USA
[‡]College of Chemistry and Chemical Engineering, iCHEM, State Key Laboratory of Physical Chemistry of Solid Surface, Xiamen University, Xiamen 361005, People's Republic of China

Supporting Information Placeholder

ABSTRACT: Here we report the design of an enzyme-inspired metal-organic framework (MOF), **1**-OTf-Ir, by installing strong Lewis acid and photoredox sites in engineered mesopores. Al-MOF (**1**) with mixed 2,2'-bipyridyl-5,5-dicarboxylate (dcbpy) and 1,4-benzenediacrylate (pdac) ligands was oxidized with ozone and then tiflated to generate strongly Lewis acidic Al-OTf sites in the mesopores, followed by the installation of $[Ir(ppy)_2(dcbpy)]^+$ (ppy = 2-phenylpyridine) sites to afford **1**-OTf-Ir with both Lewis acid and photoredox sites. **1**-OTf-Ir effectively catalyzed reductive cross-coupling of *N*-hydroxyphthalimide esters or aryl bromomethyl ketones with vinyl- or alkynyl-azaarenes to afford new azaarene derivatives. **1**-OTf-Ir enabled catalytic synthesis of anticholinergic drugs Pheniramine and Chlorpheniramine.

Functionalization of azaarene derivatives is of great significance due to their prevalence in bioactive and drug molecules.[1-4] Transition metal catalysts are typically ineffective for the modification of azaarene derivatives owing to strong coordination of azaarenes to metal centers.[5-6] Photoredox catalysis presents an alternative solution to functionalizing azaarene derivatives by generating active open-shell species via single electron transfer.[7-8] For example, the addition of photoredox-generated radicals to vinylpyridines has provided access to new functionalized pyridines.[9-11] Despite the potential of azaarene derivatives as "privileged" scaffolds in drug discovery,[2] photocatalytic transformations of azaarenes have not been widely studied.

As a versatile family of porous molecular materials, metal-organic frameworks (MOFs) have been explored for many applications,[12-16] including gas storage and separation,[17] drug delivery,[18-19] sensing,[20] solar energy conversion,[21] and heterogeneous catalysis.[22-30] Although MOFs have been extensively explored as single-site solid catalysts,[31-34] few multi-functional MOFs with two or more catalytic centers have been rationally designed.[35-39] The ability to hierarchically install multiple active sites in a MOF provides a unique opportunity to engineer enzyme-inspired cooperative catalysts that cannot be obtained in homogeneous solutions or on traditional heterogeneous supports.[40-41]

Enzymes use active sites in three-dimensional grooves or pockets to catalyze chemical transformations.[42-44] The active sites typically comprise multiple functional units that are broadly categorized as binding centers and catalytic centers.[45-47] Binding centers anchor substrates or intermediates to facilitate their conversion to products by catalytic centers. Synergistic cooperation between these functional units is responsible for the extremely high activity and selectivity of enzymes.

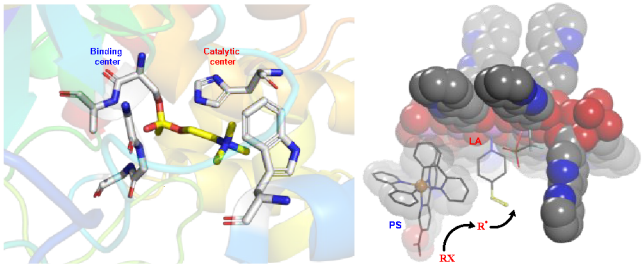

Figure 1. Comparison between an enzyme active site with binding center and catalytic center (left) and an engineered mesopore in **1**-OTf-Ir with Lewis acid as binding center and Ir-photosensitizer as catalytic center (right).

Here we report the design of an enzyme-inspired MOF, **1**-OTf-Ir, by constructing strong Lewis acid sites as binding centers and photoredox sites as catalytic centers in engineered mesopores.[48-53] Ozonolysis of Al-MOF (**1**) with mixed 2,2'-bipyridyl-5,5-dicarboxylate (dcbpy) and 1,4-benzenediacrylate (pdac) ligands followed by triflation generated Lewis acidic Al-OTf sites in the mesopores. Subsequent installation of $[Ir(ppy)_2(dcbpy)]^+$ (ppy = 2-phenylpyridine) sites afforded **1**-OTf-Ir with both Lewis acidic sites and photoredox sites. **1**-OTf-Ir effectively catalyzed reductive cross-coupling of *N*-hydroxyphthalimide esters or aryl bromomethyl ketones with vinyl- or alkynyl-azaarenes to afford new azaarene derivatives. **1**-OTf-Ir also provided alternative routes to anticholinergic drugs Pheniramine and Chlorpheniramine.

MOF **1** of the formula $Al(OH)(dcbpy)_{0.8}(pdac)_{0.2}$ was prepared through a solvothermal reaction of $Al(NO_3)_3$, H_2(dcbpy), and H_2(pdac) in N,N-dimethylformamide (DMF) as previously reported (Scheme S1).[54-56] Ozonolysis of **1** completely removed the pdac ligands to afford **1**-OH with a formula of $Al(OH)(dcbpy)_{0.8}(OH)_{0.4}(H_2O)_{0.4}$ (Scheme S2).[57-58] Treatment of **1**-OH with Me_3Si-OTf in benzene afforded **1**-OTf with a formula of $Al(OH)(dcbpy)_{0.8}(OTf)_{0.40}$ (Scheme S3).[49] Transmission electron microscopy (TEM) and scanning electron microscopy (SEM) imaging showed **1**-OH and **1**-OTf maintained the plate-like morphology of **1** (Figures 2c, S3 and S7) while powder X-ray diffraction (PXRD) analysis indicated **1**, **1**-OH, and **1**-OTf possessed a similar structure to DUT-5 and MOF-253 (Figure 2b). **1** and **1**-OH exhibited similar type I N_2 sorption isotherms with Brunauer-Emmett-Teller (BET) surface areas of 1381 m^2/g and 1052 m^2/g, respectively, and pore sizes of ~1.0 nm and 1.0-12.0 nm, respectively (Figures S4 and S8).

Treatment of **1**-OTf with $[Ir(ppy)_2Cl]_2$ afforded **1**-OTf-Ir with Ir-photosensitizer (Ir-PS) loadings of 10.4 mol% as determined by ^1H NMR spectra of digested **1**-OTf-Ir (Figures 2a and S10). In contrast, Ir-PS could not be loaded into **1** (Figure S20) because the size of $[Ir(ppy)_2Cl]_2$ (~ 1.4 nm) is larger than the pore size of **1** (~1.0 nm). The highest Ir-PS loading of 17.3 mol% is slightly lower than the density (20.0 mol%) of mesopores (Figure S16), supporting the installation of Ir-PSs inside the mesopores.

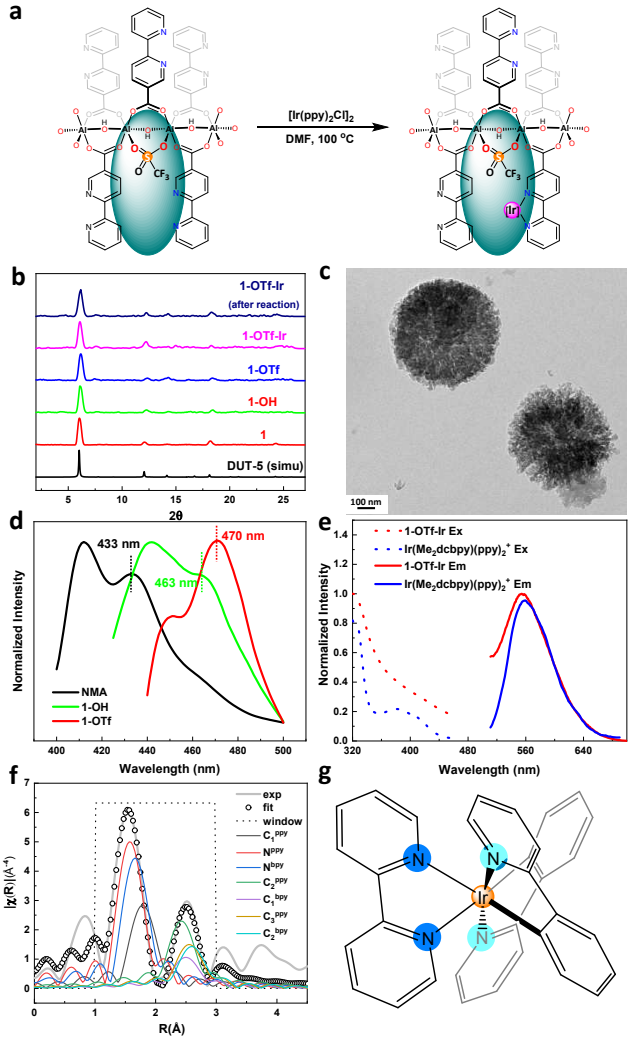

Figure 2. (a) Synthetic route to **1**-OTf-Ir. (b) PXRD patterns of **1**, **1**-OH, **1**-OTf, and **1**-OTf-Ir (pristine and after catalysis) in comparison to the simulated pattern for DUT-5. (c) TEM image of **1**-OTf-Ir. (d) Fluorescence spectra of free NMA (black) and NMA bound to **1**-OH (green) and **1**-OTf (red) in MeCN at 298 K. (e) Normalized excitation and emission spectra of **1**-OTf-Ir and $Ir(Me_2dcbpy)(ppy)_2^+$. (f) EXAFS fitting of **1**-OTf-Ir. (g) Molecular model of $Ir(bpy)(ppy)_2^+$.

1-OTf-Ir retained the crystallinity of **1** as shown by their similar PXRD patterns (Figure 2b). Lewis acidity of **1**-OH and **1**-OTf was determined by N-methylacridone (NMA) fluorescence method.[59-60] Upon coordinating to **1**-OTf, the λ_{max} of NMA emission shifted from 433 nm to 470 nm, (Figure 2d, red). In comparison, **1**-OH only shifted the λ_{max} of NMA emission to 463 nm (Figure 2d, green). Triflation of OH/OH_2 moieties thus significantly enhanced Lewis acidity of **1**-OTf. UV-Vis and luminescence spectra (Figures 2e) of **1**-OTf-Ir exhibited characteristic absorption, excitation, and emission properties of $Ir(Me_2dcbpy)(ppy)_2Cl$. The Extended X-ray absorption fine structure (EXAFS) feature of Ir centers in **1**-OTf-Ir was well fit to the $Ir(bpy)(ppy)_2^+$ structure to afford nearly identical coordination geometry (Figures 2f and 2g). Each Ir center in **1**-OTf-Ir coordinates to two ppy and one bpy ligand in an octahedral geometry with an Ir-N^{ppy} bond length of 1.96 Å, an Ir-C^{ppy} bond length of 2.18 Å, and an Ir-N^{bpy} bond length of 2.05 Å.

We surmised that Ir-PSs and Lewis acidic sites in the mesopores of **1**-OTf-Ir could work synergistically to catalyze new reactions in an enzyme-inspired fashion. We tested this bioinspired photocatalytic strategy on reductive cross-coupling of *N*-hydroxyphthalimide esters with vinyl- or alkynyl-azaarenes. At 0.5 mol% **1**-OTf-Ir loading (based on Lewis acid sites), pentanyl *N*-hydroxyphthalimide (NHP) ester (**1a**) and 4-vinylpyridine (**2a**) coupled in the presence of Hantzsch ester (HEH) reductant in CH_3CN under blue LED irradiation (400-500 nm) at room temperature to afford **1c** in 90% yield in 6 h (standard condition, entry 1, Table 1). At the same Lewis acid loading, **1**-OTf-Ir with low (4.5 mol%) and high (17.3 mol%) Ir-PS loadings produced **1c** in lower yields (entries 2 and 3, Table 1). Reactions in 1,2-dichloroethane (DCE), toluene, and dimethoxyethane (DME) afforded **1c** in lower yields (entries 4-6, Table 1). Reducing the amount of **1a** to 1.5 equiv gave **1c** in 77% yield (entry 7, Table 1). Without light or **1**-OTf-Ir, no product was observed (entries 8 and 9, Table 1). The use of $Ir(Me_2dcbpy)(ppy)_2Cl$ and $Al(OTf)_3$ as the homogeneous control generated **1c** in 16% yield (Scheme S7).

Table 1. Optimization of reaction conditions.[a]

Entry	Variations from the '**standard**' conditions	**1c** (%)[b]
1	No variation	90
2	MOF **1-OTf-Ir**-low instead of MOF **1-OTf-Ir**	38
3	MOF **1-OTf-Ir**-high instead of MOF **1-OTf-Ir**	61
4	DCE instead of CH_3CN	50
5	Toluene instead of CH_3CN	45
6	DME instead of CH_3CN	58
7	**1a** (1.5 equiv)	77
8	Without light	none
9	Without MOF **1-OTf-Ir**	trace
10	MOF **1-OH-Ir** instead of MOF **1-OTf-Ir**	10
11	MOF **1-OTf** instead of MOF **1-OTf-Ir**	8

[a] Reactions were conducted at 0.1 mmol scale. [b] GC yields.

A variety of redox-active NHP esters were examined for reductive cross-coupling reactions under standard conditions (Table 2). Primary, secondary, and tertiary alkyl NHP esters underwent cross-couplings with 4-vinylpyridine to afford **1c**-**4c** in 85%-90% isolated yields. Sterically demanding adamantyl group was tolerated to afford **5c** in 71% yield. NHP esters bearing heterocycles (tetrahydrofuran and pyrrolidine) worked well to afford **6c** and **7c** in 79% and 88% isolated yields, respectively. Cyclopentenyl group was also tolerated to afford **8c** in 70% yield.

Different vinyl-azaarenes were also tested. Cross-coupling between 2-vinylpyridine and proline-derived NHP ester gave **9c** in 51% yield. 2-(1-Phenylvinyl)pyridine and 4-(1-phenylvinyl)-pyridine served as competent coupling partners to produce **10c** and

11c in 78% and 94% isolated yields, respectively. The use of 2-vinylquinoline afforded **12c** in 71% yield.

We also investigated reductive cross-coupling of NHP esters with alkynyl-azaarenes under standard conditions. 3-Ethynyl-pyridine reacted with adamantyl and cyclohexyl NHP esters to afford **13c** and **14c** in 50% and 73% isolated yields, respectively. Cross-couplings of proline-derived NHP ester with 3-ethynyl-pyridine, 2-ethynylpyridine, and 5-ethynylpyrimidine afforded **15c**, **16c**, and **17c** in 95%, 87%, and 91% isolated yields, respectively. The highest turnover number of 190 was achieved for **15c**. Both Z and E isomers formed in these reactions, likely due to rapid isomerization of the vinyl radical intermediate. The Z/E ratio of cross-coupling products depended on both coupling partners and varied from 1.9/1 to 10/1. It is worth noting that several coupling products such as **5c**, **7c**, **10c** and **17c** are important scaffolds in drug molecules.[61-64]

Table 2. 1-OTf-Ir catalyzed reductive cross-coupling reactions.[a]

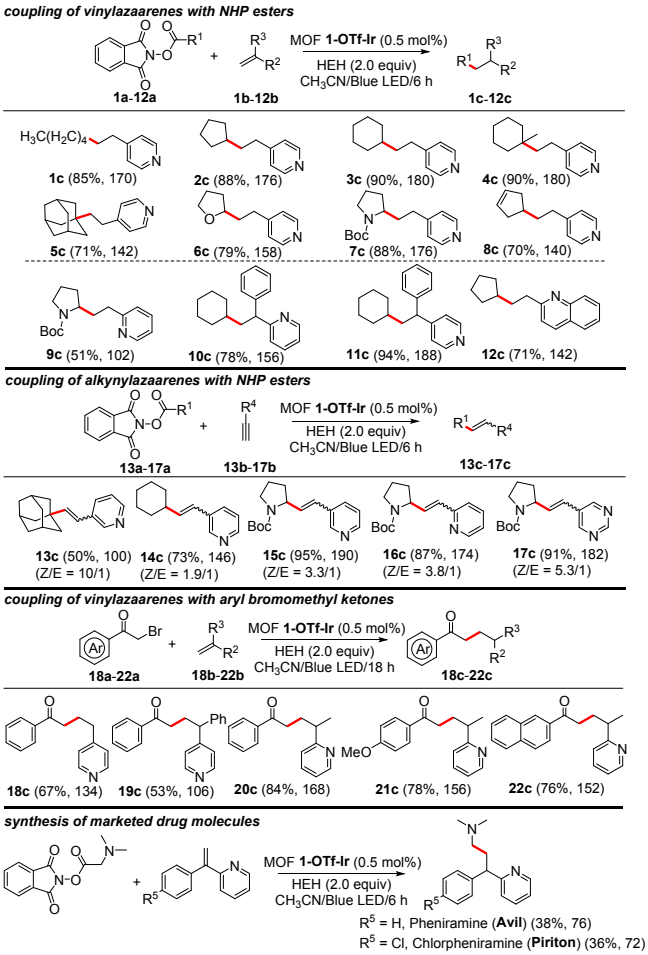

[a]Reactions were conducted at 0.1 mmol scale, yield of isolated products.

Aryl bromomethyl ketones were also used as radical precursors for reductive cross-coupling reactions. Bromoacetophenone reacted with 4-vinylpyridine, 1-phenyl-1-(4-pyridyl)ethene, and 2-isopropenylpyridine to give **18c**-**20c** in 53%-84% isolated yields. *p*-Methoxyphenacyl bromide and 2-naphthacyl bromide served as competent coupling partners to afford **21c** and **22c** in 78% and 76% isolated yields, respectively.

We tested the use of the photocatalytic reductive coupling in drug molecule synthesis. As shown in Table 2, dimethylglycine-derived NHP ester coupled with 2-(1-phenylvinyl)pyridine under standard conditions to afford Pheniramine in 38% yield. Chlorpheniramine was similarly synthesized in 36% yield.

1-OTf-Ir was stable under catalytic conditions as indicated by the retention of the PXRD pattern for the recovered MOF (Figure 2b) and the leaching of <0.1% Al and <0.1% Ir into the supernatant. **1**-OTf-Ir was recovered and used in five runs of reductive cross-coupling between 4-vinyl-pyridine and pentanyl NHP ester with no decrease in catalytic activity (Figure 3c). The optimal Lewis acid to Ir-PS ratio of 3.8 in **1**-OTf-Ir is similar to those of binding centers to catalytic centers in enzymes,[45] but much lower than those of homogeneous catalytic systems (> 10/1).[9] The excellent catalytic activity of **1**-OTf-Ir may be attributed to the pore confinement effect, which facilitates the reaction of reactive radicals and activated azaarenes in an enzyme-inspired fashion.[42]

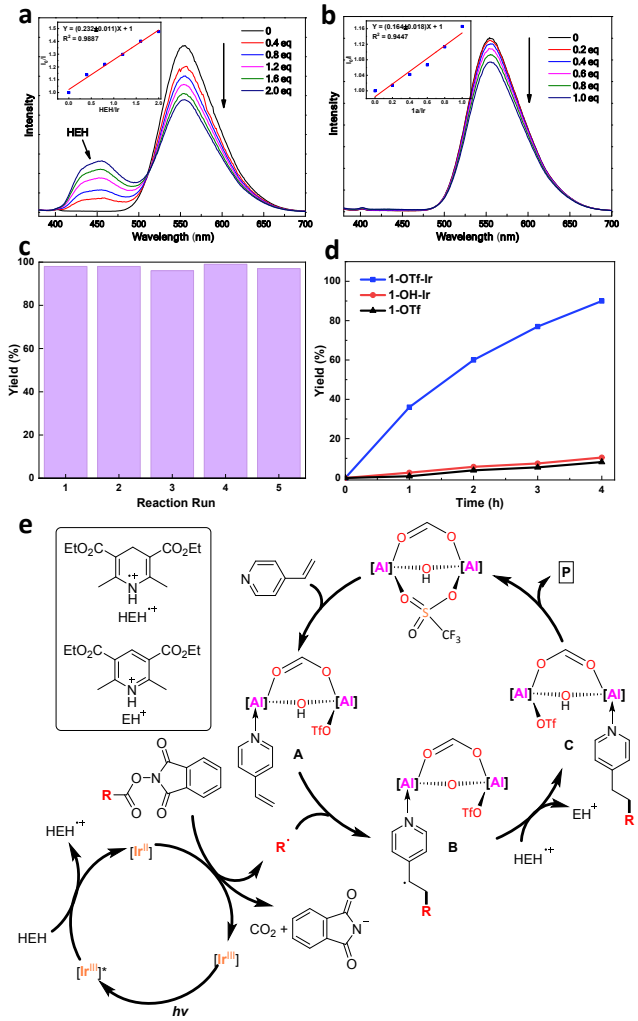

Figure 3. (a,b) Emission spectra of **1**-OTf-Ir after the addition of different amounts of HEH (a) or **1a** (b) with 365 nm excitation. Insets show plots of I_0/I of **1**-OTf-Ir as a function of equivalents of HEH (a) or **1a** (b). (c) Yields of **1c** with recovered **1**-OTf-Ir in five consecutive runs. (d) Time-dependent yields of **1c** with different catalysts. (e) Proposed reaction mechanism.

Several control experiments were conducted to shed light on the reaction mechanism. **1**-OH-Ir containing only Ir-PS gave the coupling product **1c** in 10% yield (Figure 3d). **1**-OTf with only

Lewis acidic sites catalyzed the reductive cross-coupling to afford **1c** in 8% yield (Figure 3d). These results indicate the crucial role of both PSs and strong Lewis acids. In addition, a combination of **1**-OH-Ir and **1**-OTf as the catalyst produced **1c** in 23% yield (Scheme S8), supporting the advantage of integrating both active centers in the mesopores.

Upon excitation at 365 nm, luminescence of **1**-OTf-Ir was quenched by both HEH and **1a**, but not **1b** (Figures 3a and 3b). Luminescence quenching by HEH and **1a** were well fitted to the Stern-Völmer equation to give a K_{sv}(HEH) of 0.232±0.011 and a K_{sv}(**1a**) of 0.164±0.018, suggesting preferential quenching of [Ir^{III}]* species by HEH over **1a**. In addition, radical capture by (2,2,6,6-tetramethylpiperidin-1-yl)oxyl (TEMPO) or 1,1-diphenylethene completely shut down the formation of **1c** but generated 1-pentyloxy-2,2,6,6-tetramethylpiperidine (**1d**) or 1,1-diphenylheptane (**1e**) in 26% and 91% yields, respectively (Schemes S5 and S6). This result suggests the presence of pentanyl radical in the reaction.

On the basis of these experimental results and literature precedents,[9-11] we propose a reaction mechanism as shown in Figure 3e. Reduction of photoexcited [Ir^{III}]* in by HEH furnishes $HEH^{\cdot+}$ radical cation and strongly reducing [Ir^{II}] center, which competently reduces substrates **a** to give alkyl radical and regenerate the [Ir^{III}] species. In the meantime, substrates **b** coordinates to the Lewis acidic site in the same mesopore to afford electron-deficient pyridine derivative **A** which is susceptible to attack by alkyl radical. Subsequent radical addition generates radical intermediate **B**, which undergoes hydrogen atom transfer with $HEH^{\cdot+}$ to afford Lewis acid-bound product **C** and EH^+ cation. An incoming substrate releases product **P** and restarts the catalytic cycle on the right. As the active centers are engineered into the same mesopore, the reactive intermediates are confined in the mesopore, resulting in high local concentrations to facilitate the coupling reaction.

In summary, we have engineered mesopores in the **1**-OTf-Ir MOF for the installation of strongly Lewis acid sites and Ir-PSs to perform bioinspired synergistic catalysis. **1**-OTf-Ir effectively catalyzed reductive cross-coupling of *N*-hydroxyphthalimide esters or aryl bromomethyl ketones with vinyl- or alkynyl-azaarenes to afford functionalized azaarene derivatives with turnover numbers of up to 190. **1**-OTf-Ir was also used to synthesize anticholinergic drugs Pheniramine and Chlorpheniramine. **1**-OTf-Ir significantly outperformed homogeneous and other controls as a result of the close proximity of both binding centers and catalytic centers in the mesopore which facilitates the coupling between activated vinyl- or alkyny-azaarenes and alkyl radicals. This work highlights the potential of enzyme-inspired multifunctional MOFs in synergistic catalysis.

Supporting Information

The Supporting Information is available free of charge on the ACS Publications website.

Synthesis and characterization of **1**-OTf-Ir, synergistically catalytic reactions, and mechanism study (PDF)

AUTHOR INFORMATION

Corresponding Author

wenbinlin@uchicago.edu

Author Contributions

[§]These authors contributed equally.

Notes

The authors declare no competing financial interests.

ACKNOWLEDGMENT

We thank Xuanyu Feng for experimental help. We acknowledge the National Science Foundation and the University of Chicago for founding support and the MRSEC Shared User Facilities at the University of Chicago (NSF DMR-1420709) for instrument access. XAS analysis was performed at Beamline 10-BM, supported by the Materials Research Collaborative Access Team (MRCAT). Use of the Advanced Photon Source, an Office of Science User Facility operated for the U.S. DOE Office of Science by ANL, was supported by the U.S. DOE under Contract No. DE-AC02-06CH11357.

REFERENCES

1. Kiuru, P.; Yli-Kauhaluoma, J., Pyridine and Its Derivatives. *Heterocycles in Natural Product Synthesis* **2011**, 267-297.
2. Thiel, O., Heterocyclic Chemistry in Drug Discovery. Edited by Jie Jack Li. *Angew. Chem. Int. Ed.* **2013,** *52* (51), 13515-13515.
3. Goetz, A. E.; Garg, N. K., Regioselective reactions of 3,4-pyridynes enabled by the aryne distortion model. *Nat. Chem.* **2013,** *5* (1), 54-60.
4. Vitaku, E.; Smith, D. T.; Njardarson, J. T., Analysis of the Structural Diversity, Substitution Patterns, and Frequency of Nitrogen Heterocycles among U.S. FDA Approved Pharmaceuticals. *J. Med. Chem.* **2014,** *57* (24), 10257-10274.
5. Seregin, I. V.; Gevorgyan, V., Direct transition metal-catalyzed functionalization of heteroaromatic compounds. *Chem. Soc. Rev.* **2007,** *36* (7), 1173-1193.
6. Feuerstein, M.; Doucet, H.; Santelli, M., Efficient coupling of heteroaryl halides with arylboronic acids in the presence of a palladium–tetraphosphine catalyst. *J. Organomet. Chem.* **2003,** *687* (2), 327-336.
7. Prier, C. K.; Rankic, D. A.; MacMillan, D. W. C., Visible Light Photoredox Catalysis with Transition Metal Complexes: Applications in Organic Synthesis. *Chem. Rev.* **2013,** *113* (7), 5322-5363.
8. Skubi, K. L.; Blum, T. R.; Yoon, T. P., Dual Catalysis Strategies in Photochemical Synthesis. *Chem. Rev.* **2016,** *116* (17), 10035-10074.
9. Lee, K. N.; Lei, Z.; Ngai, M.-Y., β-Selective Reductive Coupling of Alkenylpyridines with Aldehydes and Imines via Synergistic Lewis Acid/Photoredox Catalysis. *J. Am. Chem. Soc.* **2017,** *139* (14), 5003-5006.
10. Trowbridge, A.; Reich, D.; Gaunt, M. J., Multicomponent synthesis of tertiary alkylamines by photocatalytic olefin-hydroaminoalkylation. *Nature* **2018,** *561* (7724), 522-527.
11. Cao, K.; Tan, S. M.; Lee, R.; Yang, S.; Jia, H.; Zhao, X.; Qiao, B.; Jiang, Z., Catalytic Enantioselective Addition of Prochiral Radicals to Vinylpyridines. *J. Am. Chem. Soc.* **2019,** *141* (13), 5437-5443.
12. Furukawa, H.; Cordova, K. E.; O'Keeffe, M.; Yaghi, O. M., The Chemistry and Applications of Metal-Organic Frameworks. *Science* **2013,** *341* (6149), 1230444.
13. Long, J. R.; Yaghi, O. M., The pervasive chemistry of metal–organic frameworks. *Chem. Soc. Rev.* **2009,** *38* (5), 1213-1214.
14. Lu, K.; Aung, T.; Guo, N.; Weichselbaum, R.; Lin, W., Nanoscale Metal–Organic Frameworks for Therapeutic, Imaging, and Sensing Applications. *Adv. Mater.* **2018,** *30* (37), 1707634.

15. Zhang, Y.; Wu, J.; Cui, S.; Wei, W.; Chen, W.; Pang, R.; Wu, Z.; Mi, L., Organosulfonate Counteranions—A Trapped Coordination Polymer as a High-Output Triboelectric Nanogenerator Material for Self-Powered Anticorrosion. *Chem. Eur. J.* **2020,** *26* (3), 584-591.
16. Wen, R.; Guo, J.; Yu, A.; Zhai, J.; Wang, Z. l., Humidity-Resistive Triboelectric Nanogenerator Fabricated Using Metal Organic Framework Composite. *Adv. Funct. Mater.* **2019,** *29* (20), 1807655.
17. Lin, R.-B.; Xiang, S.; Xing, H.; Zhou, W.; Chen, B., Exploration of porous metal–organic frameworks for gas separation and purification. *Coord. Chem. Rev.* **2019,** *378*, 87-103.
18. Horcajada, P.; Gref, R.; Baati, T.; Allan, P. K.; Maurin, G.; Couvreur, P.; Férey, G.; Morris, R. E.; Serre, C., Metal–Organic Frameworks in Biomedicine. *Chem. Rev.* **2012,** *112* (2), 1232-1268.
19. Duan, X.; Chan, C.; Lin, W., Nanoparticle-Mediated Immunogenic Cell Death Enables and Potentiates Cancer Immunotherapy. *Angew. Chem. Int. Ed.* **2019,** *58* (3), 670-680.
20. Hu, Z.; Deibert, B. J.; Li, J., Luminescent metal–organic frameworks for chemical sensing and explosive detection. *Chem. Soc. Rev.* **2014,** *43* (16), 5815-5840.
21. Chueh, C.-C.; Chen, C.-I.; Su, Y.-A.; Konnerth, H.; Gu, Y.-J.; Kung, C.-W.; Wu, K. C. W., Harnessing MOF materials in photovoltaic devices: recent advances, challenges, and perspectives. *J. Mater. Chem. A* **2019,** *7* (29), 17079-17095.
22. Ma, L.; Abney, C.; Lin, W., Enantioselective catalysis with homochiral metal–organic frameworks. *Chem. Soc. Rev.* **2009,** *38* (5), 1248-1256.
23. Yoon, M.; Srirambalaji, R.; Kim, K., Homochiral Metal–Organic Frameworks for Asymmetric Heterogeneous Catalysis. *Chem. Rev.* **2012,** *112* (2), 1196-1231.
24. Zhang, T.; Lin, W., Metal–organic frameworks for artificial photosynthesis and photocatalysis. *Chem. Soc. Rev.* **2014,** *43* (16), 5982-5993.
25. Dhakshinamoorthy, A.; Li, Z.; Garcia, H., Catalysis and photocatalysis by metal organic frameworks. *Chem. Soc. Rev.* **2018,** *47* (22), 8134-8172.
26. Zhu, L.; Liu, X.-Q.; Jiang, H.-L.; Sun, L.-B., Metal–Organic Frameworks for Heterogeneous Basic Catalysis. *Chem. Rev.* **2017,** *117* (12), 8129-8176.
27. Li, G.; Zhao, S.; Zhang, Y.; Tang, Z., Metal–Organic Frameworks Encapsulating Active Nanoparticles as Emerging Composites for Catalysis: Recent Progress and Perspectives. *Adv. Mater.* **2018,** *30* (51), 1800702.
28. Yang, D.; Gates, B. C., Catalysis by Metal Organic Frameworks: Perspective and Suggestions for Future Research. *ACS Catal.* **2019,** *9* (3), 1779-1798.
29. Pascanu, V.; González Miera, G.; Inge, A. K.; Martín-Matute, B., Metal–Organic Frameworks as Catalysts for Organic Synthesis: A Critical Perspective. *J. Am. Chem. Soc.* **2019,** *141* (18), 7223-7234.
30. Bavykina, A.; Kolobov, N.; Khan, I. S.; Bau, J. A.; Ramirez, A.; Gascon, J., Metal–Organic Frameworks in Heterogeneous Catalysis: Recent Progress, New Trends, and Future Perspectives. *Chem. Rev.* **2020**, DOI: 10.1021/acs.chemrev.9b00685.
31. Ma, L.; Falkowski, J. M.; Abney, C.; Lin, W., A series of isoreticular chiral metal–organic frameworks as a tunable platform for asymmetric catalysis. *Nat. Chem.* **2010,** *2* (10), 838-846.
32. Rogge, S. M. J.; Bavykina, A.; Hajek, J.; Garcia, H.; Olivos-Suarez, A. I.; Sepúlveda-Escribano, A.; Vimont, A.; Clet, G.; Bazin, P.; Kapteijn, F.; Daturi, M.; Ramos-Fernandez, E. V.; Llabrés i Xamena, F. X.; Van Speybroeck, V.; Gascon, J., Metal–organic and covalent organic frameworks as single-site catalysts. *Chem. Soc. Rev.* **2017,** *46* (11), 3134-3184.
33. Jiao, L.; Wang, Y.; Jiang, H.-L.; Xu, Q., Metal–Organic Frameworks as Platforms for Catalytic Applications. *Adv. Mater.* **2018,** *30* (37), 1703663.
34. Drake, T.; Ji, P.; Lin, W., Site Isolation in Metal–Organic Frameworks Enables Novel Transition Metal Catalysis. *Acc. Chem. Res.* **2018,** *51* (9), 2129-2138.
35. Gu, X.; Lu, Z.-H.; Jiang, H.-L.; Akita, T.; Xu, Q., Synergistic Catalysis of Metal–Organic Framework-Immobilized Au–Pd Nanoparticles in Dehydrogenation of Formic Acid for Chemical Hydrogen Storage. *J. Am. Chem. Soc.* **2011,** *133* (31), 11822-11825.
36. Han, Q.; He, C.; Zhao, M.; Qi, B.; Niu, J.; Duan, C., Engineering Chiral Polyoxometalate Hybrid Metal–Organic Frameworks for Asymmetric Dihydroxylation of Olefins. *J. Am. Chem. Soc.* **2013,** *135* (28), 10186-10189.
37. Huang, Y.-B.; Liang, J.; Wang, X.-S.; Cao, R., Multifunctional metal–organic framework catalysts: synergistic catalysis and tandem reactions. *Chem. Soc. Rev.* **2017,** *46* (1), 126-157.
38. Wu, C.-D.; Zhao, M., Incorporation of Molecular Catalysts in Metal–Organic Frameworks for Highly Efficient Heterogeneous Catalysis. *Adv. Mater.* **2017,** *29* (14), 1605446.
39. Zhu, Y.-Y.; Lan, G.; Fan, Y.; Veroneau, S. S.; Song, Y.; Micheroni, D.; Lin, W., Merging Photoredox and Organometallic Catalysts in a Metal–Organic Framework Significantly Boosts Photocatalytic Activities. *Angew. Chem. Int. Ed.* **2018,** *57* (43), 14090-14094.
40. Zhao, M.; Ou, S.; Wu, C.-D., Porous Metal–Organic Frameworks for Heterogeneous Biomimetic Catalysis. *Acc. Chem. Res.* **2014,** *47* (4), 1199-1207.
41. Nath, I.; Chakraborty, J.; Verpoort, F., Metal organic frameworks mimicking natural enzymes: a structural and functional analogy. *Chem. Soc. Rev.* **2016,** *45* (15), 4127-4170.
42. Ringe, D.; Petsko, G. A., How Enzymes Work. *Science* **2008,** *320* (5882), 1428.
43. Bugg, T. D. H., Enzymes Are Wonderful Catalysts. *Introduction to Enzyme and Coenzyme Chemistry* **2012**, 26-49.
44. Pravda, L.; Berka, K.; Svobodová Vařeková, R.; Sehnal, D.; Banáš, P.; Laskowski, R. A.; Koča, J.; Otyepka, M., Anatomy of enzyme channels. *BMC Bioinform.* **2014,** *15* (1), 379.
45. Structural Components of Enzymes. *Enzymes* **2000**, 42-75.
46. Koshland Jr, D. E., The Key − Lock Theory and the Induced Fit Theory. *Angew. Chem. Int. Ed.* **1995,** *33* (23 - 24), 2375-2378.
47. Sullivan, S. M.; Holyoak, T., Enzymes with lid-gated active sites must operate by an induced fit mechanism instead of conformational selection. *PNAS* **2008,** *105* (37), 13829.
48. Qiu, L.-G.; Xu, T.; Li, Z.-Q.; Wang, W.; Wu, Y.; Jiang, X.; Tian, X.-Y.; Zhang, L.-D., Hierarchically Micro- and Mesoporous Metal–Organic Frameworks with Tunable Porosity. *Angew. Chem. Int. Ed.* **2008,** *47* (49), 9487-9491.
49. Zhao, D.; Timmons, D. J.; Yuan, D.; Zhou, H.-C., Tuning the Topology and Functionality of Metal−Organic Frameworks by Ligand Design. *Acc. Chem. Res.* **2011,** *44* (2), 123-133.
50. Yue, Y.; Qiao, Z.-A.; Fulvio, P. F.; Binder, A. J.; Tian, C.; Chen, J.; Nelson, K. M.; Zhu, X.; Dai, S., Template-Free Synthesis of Hierarchical Porous Metal–Organic Frameworks. *J. Am. Chem. Soc.* **2013,** *135* (26), 9572-9575.
51. Kim, Y.; Yang, T.; Yun, G.; Ghasemian, M. B.; Koo, J.; Lee, E.; Cho, S. J.; Kim, K., Hydrolytic Transformation of Microporous Metal–Organic Frameworks to Hierarchical

Micro- and Mesoporous MOFs. *Angew. Chem. Int. Ed.* **2015,** *54* (45), 13273-13278.
52. Cai, G.; Jiang, H.-L., A Modulator-Induced Defect-Formation Strategy to Hierarchically Porous Metal–Organic Frameworks with High Stability. *Angew. Chem. Int. Ed.* **2017,** *56* (2), 563-567.
53. Chang, G.-G.; Ma, X.-C.; Zhang, Y.-X.; Wang, L.-Y.; Tian, G.; Liu, J.-W.; Wu, J.; Hu, Z.-Y.; Yang, X.-Y.; Chen, B., Construction of Hierarchical Metal–Organic Frameworks by Competitive Coordination Strategy for Highly Efficient CO2 Conversion. *Adv. Mater.* **2019,** *31* (52), 1904969.
54. Senkovska, I.; Hoffmann, F.; Fröba, M.; Getzschmann, J.; Böhlmann, W.; Kaskel, S., New highly porous aluminium based metal-organic frameworks: Al(OH)(ndc) (ndc=2,6-naphthalene dicarboxylate) and Al(OH)(bpdc) (bpdc=4,4′-biphenyl dicarboxylate). *Microporous Mesoporous Mater.* **2009,** *122* (1), 93-98.
55. Bloch, E. D.; Britt, D.; Lee, C.; Doonan, C. J.; Uribe-Romo, F. J.; Furukawa, H.; Long, J. R.; Yaghi, O. M., Metal Insertion in a Microporous Metal−Organic Framework Lined with 2,2′-Bipyridine. *J. Am. Chem. Soc.* **2010,** *132* (41), 14382-14384.
56. Song, Y.; Feng, X.; Chen, J. S.; Brzezinski, C.; Xu, Z.; Lin, W., Multistep Engineering of Synergistic Catalysts in a Metal–Organic Framework for Tandem C–O Bond Cleavage. *J. Am. Chem. Soc.* **2020**.
57. Albalad, J.; Xu, H.; Gándara, F.; Haouas, M.; Martineau-Corcos, C.; Mas-Ballesté, R.; Barnett, S. A.; Juanhuix, J.; Imaz, I.; Maspoch, D., Single-Crystal-to-Single-Crystal Postsynthetic Modification of a Metal–Organic Framework via Ozonolysis. *J. Am. Chem. Soc.* **2018,** *140* (6), 2028-2031.
58. Guillerm, V.; Xu, H.; Albalad, J.; Imaz, I.; Maspoch, D., Postsynthetic Selective Ligand Cleavage by Solid–Gas Phase Ozonolysis Fuses Micropores into Mesopores in Metal–Organic Frameworks. *J. Am. Chem. Soc.* **2018,** *140* (44), 15022-15030.
59. Ji, P.; Drake, T.; Murakami, A.; Oliveres, P.; Skone, J. H.; Lin, W., Tuning Lewis Acidity of Metal–Organic Frameworks via Perfluorination of Bridging Ligands: Spectroscopic, Theoretical, and Catalytic Studies. *J. Am. Chem. Soc.* **2018,** *140* (33), 10553-10561.
60. Ohkubo, K.; Menon, S. C.; Orita, A.; Otera, J.; Fukuzumi, S., Quantitative Evaluation of Lewis Acidity of Metal Ions with Different Ligands and Counterions in Relation to the Promoting Effects of Lewis Acids on Electron Transfer Reduction of Oxygen. *J. Org. Chem.* **2003,** *68* (12), 4720-4726.
61. Blanpied, T. A.; Clarke, R. J.; Johnson, J. W., Amantadine Inhibits NMDA Receptors by Accelerating Channel Closure during Channel Block. *J. Neurosci.* **2005,** *25* (13), 3312.
62. Banister, S. D.; Wilkinson, S. M.; Longworth, M.; Stuart, J.; Apetz, N.; English, K.; Brooker, L.; Goebel, C.; Hibbs, D. E.; Glass, M.; Connor, M.; McGregor, I. S.; Kassiou, M., The Synthesis and Pharmacological Evaluation of Adamantane-Derived Indoles: Cannabimimetic Drugs of Abuse. *ACS Chem. Neurosci.* **2013,** *4* (7), 1081-1092.
63. Spande, T. F.; Garraffo, H. M.; Edwards, M. W.; Yeh, H. J. C.; Pannell, L.; Daly, J. W., Epibatidine: a novel (chloropyridyl)azabicycloheptane with potent analgesic activity from an Ecuadoran poison frog. *J. Am. Chem. Soc.* **1992,** *114* (9), 3475-3478.
64. Burckhalter, J. H.; Dixon, W. D.; Black, M. L.; Westland, R. D.; Werbel, L. M.; DeWald, H. A.; Dice, J. R.; Rodney, G.; Kaump, D. H., 2-(2-Pyridyl)-1,2-diarylalkanols as Hypocholesteremic Agents. *J. Med. Chem.* **1967,** *10* (4), 565-575.

TOC Graphic